7-25-2005

Real-Space Electron Transfer in III-Nitride Metal-Oxide-Semiconductor-Heterojunction Structures

S. Saygi

A. Koudymov

V. Adivarahan

J. Yang

Grigory Simin
University of South Carolina - Columbia, simin@engr.sc.edu

See next page for additional authors

Publication Info

Published in *Applied Physics Letters*, Volume 87, Issue 4, 2005, pages #043505-.

Saygi, S., Koudymov, A., Adivarahan, V., Yang, J., Simin, G., Khan, M. A., Deng, J., Gaska, R., & Shur, M. S. (25 July 2005). Real-Space Electron Transfer in III-Nitride Metal-Oxide-Semiconductor-Heterojunction Structures. Applied Physics Letters, 87 (4), #043505. http://dx.doi.org/10.1063/1.2001745

Real-space electron transfer in III-nitride metal-oxide-semiconductor-heterojunction structures

S. Saygi, A. Koudymov, V. Adivarahan, J. Yang, G. Simin, M. Asif Khan, J. Deng, R. Gaska, and M. S. Shur

Citation: Applied Physics Letters **87**, 043505 (2005); doi: 10.1063/1.2001745
View online: http://dx.doi.org/10.1063/1.2001745
View Table of Contents: http://scitation.aip.org/content/aip/journal/apl/87/4?ver=pdfcov
Published by the AIP Publishing

Real-space electron transfer in III-nitride metal-oxide-semiconductor-heterojunction structures

S. Saygi, A. Koudymov, V. Adivarahan, J. Yang, G. Simin,[a] and M. Asif Khan
Department of Electrical Engineering, University of South Carolina, Columbia, South Carolina 29208

J. Deng and R. Gaska
Sensor Electronic Technology, Inc., 1195 Atlas Road, Columbia, South Carolina 29209

M. S. Shur
Department of Electrical, Computer and Systems Engineering, and Broadband Center, Rensselaer Polytechnic Institute, Troy, New York 12180

(Received 18 February 2005; accepted 13 June 2005; published online 20 July 2005)

The real-space transfer effect in a SiO_2/AlGaN/GaN metal-oxide-semiconductor heterostructure (MOSH) from the two-dimensional (2D) electron gas at the heterointerface to the oxide-semiconductor interface has been demonstrated and explained. The effect occurs at high positive gate bias and manifests itself as an additional step in the capacitance-voltage (*C-V*) characteristic. The real-space transfer effect limits the achievable maximum 2D electron gas density in the device channel. We show that in MOSH structures the maximum electron gas density exceeds up to two times that at the equilibrium (zero bias) condition. Correspondingly, a significant increase in the maximum channel current (up to two times compared to conventional Schottky-gate structures) can be achieved. The real-space charge transfer effect in MOSH structures also opens up a way to design novel devices such as variable capacitors, multistate switches, memory cells, etc. © *2005 American Institute of Physics*. [DOI: 10.1063/1.2001745]

Nitride-based field effect transistors using metal-oxide-semiconductor-heterojunction (MOSH) structures (MOSHFETs) over AlGaN/GaN or AlGaN/InGaN/GaN heterojunctions[1–5] demonstrated a superior performance compared to regular Schottky-gate devices due to the unique properties of the insulated gate design. Their advantages include extremely low gate currents, large gate voltage swings, high maximum channel saturation currents, and higher and much more stable rf powers. One of the key features of MOSHFETs that distinguishes them from Schottky-based heterostructure field effect transistors (HFETs) is their ability to operate at high positive gate biases. The channel current of MOSHFETs keeps increasing with the gate bias far beyond the voltage at which the gate current in conventional HFETs increases sharply.[4] As a result, the MOSHFET channel current may significantly (up to two times) exceed that of a conventional HFET. As the gate bias goes more positive, the channel current of MOSHFET saturates, although the gate leakage current remains negligibly low. The mechanism limiting the channel current and physical processes under the gate of MOSH structures has not been analyzed in detail. In this letter, we present the study of the charge accumulation in the SiO_2/AlGaN/GaN MOSH structures at high positive biases. Our experimental data and simulation results show that when the forward bias exceeds a certain critical value, the real-space electron transfer from the two-dimensional (2D) channel to the SiO_2-AlGaN barrier interface takes place. This effect limits the maximum electron concentration in the 2D channel to approximately 1.8×10^{13} cm^{-2}, which is significantly higher than what can be achieved for undoped Schottky-based HFETs. The mobility-concentration dependencies extracted from our experimental data show that the 2D electron mobility remains high even beyond the onset of the real-space transfer. The simulations show that at high enough gate bias, the real-space transfer effects may result in very high densities of the transferred electrons and in a significant additional capacitance modulation. This opens up a way to design novel devices based on the real-space transfer in MOSH structures, such as variable capacitors [similar to those demonstrated previously on Si (Ref. 6) and SiC (Ref. 7)], switches,[8–10] and memory cells.

The nitride-based MOSH structure (see inset in Fig. 2) consists of a thin dielectric layer deposited over AlGaN/GaN heterojunction and capped with a metal electrode (the gate). The experimental MOSH structures for this study were fabricated over nominally undoped AlGaN/GaN heterojunctions, grown on sapphire substrates similar to that reported in (Ref. 5). The sheet resistance measured using on-wafer rf mapping system, was $R_{SH}\approx340$ Ω. The Ni/Au gate electrode size was 20×200 μm^2. The dielectric layer was obtained by depositing an ~120 Å layer of SiO_2 using plasma enhanced chemical vapor deposition (PECVD) system. Using two adjacent Ti/Al/Ti/Au source and drain ohmic contacts, the MOSH structure was characterized as a "fat" (very long gate) MOSHFET. The sheet electron concentration in the 2D gas channel at zero gate bias was $N_S\approx10^{13}$ cm^{-2}.

The capacitance-voltage (*C-V*) characteristic of the MOSHFET measured at 1 MHz is shown in Fig. 1. We also show in the figure the *C-V* characteristic of Schottky-based metal-semiconductor (MS) structure fabricated using the same processes except masking the source-drain area during the dielectric deposition. Since at zero gate bias both the extracted 2D gas concentration and the drain saturation current are the same for MOSH and MS structures, the threshold voltage of the MOSH structure, i.e., the voltage applied to

[a]Electronic mail: simin@engr.sc.edu

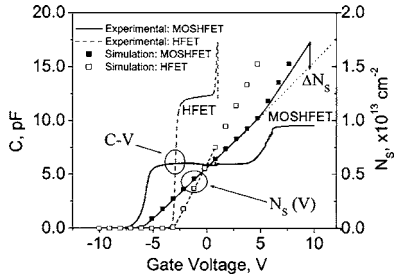

FIG. 1. *C-V* characteristics and sheet electron concentration of a 20 $\times 200\ \mu m^2$ SiO_2/AlGaN/GaN MOSH structure. Solid lines: MOSH structure; dashed lines: Schottky-gate heterostructure. The squares represent the electron concentration simulation. The amplitude for the *C-V* measurements is 10 mV. The *C-V* characteristics are frequency independent in the range of 10 kHz to 1 MHz. ΔN_S shows the sheet concentration at the SiO_2/AlGaN interface.

the gate to fully deplete the surface charge Q_S of the 2D gas layer is related to that of Schottky gate as follows:[5]

$$Q_S = qN_S = C_{\mathrm{MOSH}} \times V_{\mathrm{TMOSH}} = C_{\mathrm{MS}} \times V_{\mathrm{TMS}}. \tag{1}$$

Here N_S is the electron sheet density in the 2D gas channel, C_{MOSH} and C_{MS} are the capacitances of the MOSH and Schottky gate structures, and V_{TMOSH} and V_{TMS} are the corresponding threshold voltages. According to (1), the threshold voltages of MOSH and heterojunction structures must scale inversely proportional to their capacitances. For the MOSH structure shown in the inset of Fig. 1, $V_{\mathrm{TMOSH}}/V_{\mathrm{TMS}} \approx C_{\mathrm{MS}}/C_{\mathrm{MOSH}} \approx 2$.

When the gate bias is below the threshold, the 2D electron density is nearly zero and the capacitance of the MOSH structure is very low, corresponding to that of a planar capacitor formed by the gate electrode and the 2D gas layer outside the gate (see Fig. 2). As the gate bias increases well above the threshold voltage, the electrons under the gate form a highly conductive layer and the capacitance quickly reaches the value

$$C_{\mathrm{MOSH}} = \frac{\varepsilon_0 \varepsilon_B}{d_B}\left(1 + \frac{d_{\mathrm{OX}}}{d_B}\frac{\varepsilon_B}{\varepsilon_{\mathrm{OX}}}\right)^{-1},$$

where ε_B, $\varepsilon_{\mathrm{OX}}$, d_B, and d_{OX} are the dielectric permittivity and thickness of barrier (AlGaN) and oxide (SiO_2) layers, respectively. As the gate bias goes more positive, the 2D electrons start spilling over the AlGaN barrier layer. In the Schottky-based structures, the electron spillover immediately gives rise to gate leakage currents,[8] however, in the MOSH structure the gate currents are blocked by the insulating layer dielectric. The electron accumulation at the dielectric-semiconductor interface further increases the gate capacitance as seen from the *C-V* plot of Fig. 1.

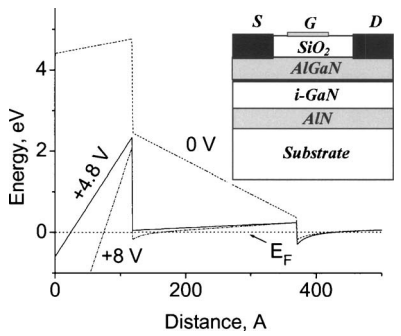

FIG. 2. Schematic structure (the inset) and the band diagram of the MOSH structure at 0, +4.8, and +8 V bias applied to the metal electrode.

The effect of real-space charge transfer can be clearly understood from the band diagrams of MOSH structure shown in the Fig. 2. The band diagram for the MOSH structure with a 120-Å thick SiO_2 layer and a 250-Å thick $Al_{0.25}Ga_{0.75}N$ barrier layer was simulated with one-dimensional (1D) Poisson solver by G. Snider.[11] Piezoelectric and spontaneous polarization was accounted for by introducing interface charges according to Ref. 12. We have found that the polarization charges at the SiO_2/AlGaN need to be partially (about 50%) compensated by the dielectric surface charges in order for the simulations to fit the experimental *C-V* and *I-V* data.

For the MOSH structure under consideration, the onset of real-space charge transfer corresponds to a positive gate bias of around +5 V, when the conduction band edge at the SiO_2/AlGaN interface crosses the Fermi level, creating an electron accumulation layer (Fig. 2). From the band diagram of Fig. 2, the critical voltage for the real-space transfer V_{RST}, can be found as

$$V_{\mathrm{RST}} = \varphi_{\mathrm{OX}} - \Delta E_{C1} + \frac{d_{\mathrm{ox}}}{\varepsilon_{\mathrm{ox}}}\left[\frac{\varepsilon_B}{d_B}(\Delta E_{c2} - 0.25) + Q\right], \tag{2}$$

where $\varphi_{\mathrm{OX}} \approx 4.4$ V is the barrier height at the metal-SiO_2 interface, $\Delta E_{C1} \approx 2.1$ V and $\Delta E_{C2} \approx 0.7$ V are the conduction band offsets at the SiO_2/AlGaN and AlGaN/GaN interfaces, correspondingly, and Q is the uncompensated charge sheet density at the SiO_2–AlGaN interface. The value of ΔE_{C2} in Eq. (2) is reduced by 0.25 V to account for the difference between the Fermi level position and the bottom of the quantum well. With the parameters of MOSH structure used in our experiments, Eq. (2) gives the estimate of the critical voltage, $V_{\mathrm{RST}} = 4.8$ V. As can be seen from Fig. 1, the experimental *C-V* characteristics show an increase of capacitance at the bias exceeding the onset of the real-space transfer $V_G \approx 4.5$ V, quite close to the value of V_{RST} found from the band diagram. From the *C-V* characteristics of Fig. 1, one can easily see that maximum capacitance measured at $V_G > V_{\mathrm{RST}}$, closely corresponds to that of plain capacitor with electrode separation equal to the dielectric thickness d_{OX}: $C_{\mathrm{RST}} = \varepsilon_0 \varepsilon_{\mathrm{OX}}/d_{\mathrm{OX}}$, where we defined C_{RST} as the capacitance in the real-space electron transfer region. Electron sheet density under the gate was extracted from the *C-V* characteristics using the expression $n_s = (1/q)\int_{-\infty}^{V_g} C dV_g$. This concentration as a function of applied bias is plotted in Fig. 1 for the MOSHFET and HFET under study. We can see that above the threshold the electron concentration increases linearly with the gate bias. For the HFET maximum sheet density $\approx 0.8 \times 10^{12}$ cm^{-2} is reached at $V_G \approx 1$ V, the forward bias resulting in sharp increase of the current through the Schottky electrode. For the MOSHFET, the dependence $n_S(V_G)$ remains nearly linear in the entire range of applied voltages, up to $V_G = +10$ V. At the gate bias exceeding the onset of the real-space transfer, n_S increases superlinearly with V_G (see Fig. 1). The value $\Delta n_s \cong C_{\mathrm{RST}} \times (V_G - V_{\mathrm{RST}})/q$ indicates the surface density of electrons accumulated at the dielectric-semiconductor interface.

To determine the 2D electron gas characteristics at high positive gate bias, we have extracted the mobility-concentration dependencies using the gate bias dependencies of gate capacitance and channel resistance.[13] To obtain the

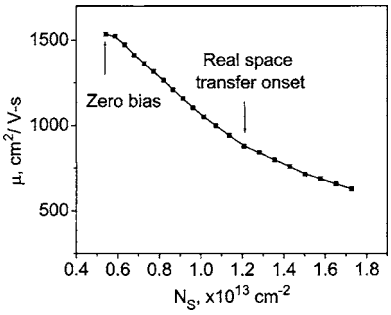

FIG. 3. Mobility-concentration dependence for the MOSH structure at high positive bias.

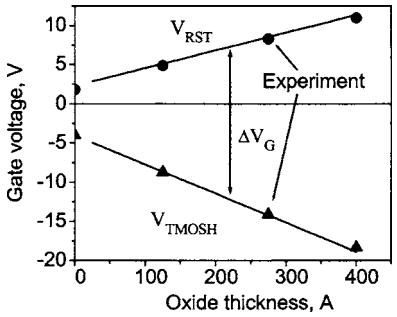

FIG. 4. MOSHFET threshold voltage and the critical voltage for the real-space transfer as a function of dielectric thickness. Solid lines: calculated. Symbols: measured on MOSHFETs with different dielectric thicknesses. The points corresponding to $d_{OX}=0$ were measured on HFET devices from the same wafer.

channel resistance-gate bias dependence we have used Gated TLM test patterns with different gate lengths. The extracted mobility-concentration profile is shown in Fig. 3. As seen, the real-space charge transfer almost does not change the slope of mobility-concentration dependence, although the mobility in the 2D gas layer is much higher than that of quasi-three-dimensional electrons at the dielectric-AlGaN interface. From this extraction, we conclude that the 2D electron gas sheet density continues increasing with the gate bias even beyond the onset of real-space transfer (shown as the dotted line in Fig. 1). Therefore, maximum achievable electron concentration in the MOSH structure significantly exceeds that under the Schottky gate.

As seen from the above consideration, the MOSH structure significantly expands the range of gate bias voltages available for transistor operation thus increasing the device linearity and output rf powers.[8,14] The available input voltage range for the MOSHFET, ΔV_{GMAX} can be estimated as $\Delta V_{GMAX}=V_{RST}+|V_{TMOSH}|$. The dependence of V_{RST} and V_{TMOSH} on the dielectric thickness plotted using the Eqs. (1) and (2) is shown in Fig. 4. In this figure, we also show the experimental points for V_{RST} and V_{TMOSH} measured using MOSHFETs with different dielectric thickness. Close correspondence to the calculated data is clearly seen.

In conclusion, we have demonstrated the effect of real-space electron transfer in the $SiO_2/AlGaN/GaN$ MOSH structures. This effect results in additional electron accumulation at the $SiO_2/AlGaN$ interface at high positive bias. Due to the absence of gate leakage currents, maximum 2D electron gas concentration in the MOSH structure used in our study was about 1.8×10^{13} cm^{-2}, nearly two times higher than that of conventional HFET fabricated on the same wafer. The real space electron transfer in MOSH structures also allows for a number of novel applications, such as high-power three-state switching capacitors, phase shifters, and memory cells.

[1]M. A. Khan, X. Hu, G. Simin, A. Lunev, J. Yang, R. Gaska, and M. S. Shur, IEEE Electron Device Lett. **21**, 63 (2000).
[2]M. A. Khan, X. Hu, G. Simin, J. Yang, R. Gaska, and M. S. Shur, Appl. Phys. Lett. **77**, 1339 (2000).
[3]C. K. Wang, S. J. Chang, Y. K. Su, Y. Z. Chiou, T. K. Lin, B. R. Huang, Phys. Status Solidi C **0, 7**, 2355 (2003).
[4]A. Koudymov, H. Fatima, G. Simin, J. Yang, M. A. Khan, A. Tarakji, X. Hu, M. S. Shur, and R. Gaska, Appl. Phys. Lett. **80**, 3216 (2002).
[5]M. Asif Khan, G. Simin, J. Yang, J. Zhang, A. Koudymov, M. S. Shur, R. Gaska, X. Hu, and A. Tarakji, IEEE MTT-S Int. Microwave Symp. Dig. **51**, 624 (2003).
[6]R. W. Brodersen, P. R. Gray, and D. A. Hodges, Proc. IEEE **67**, 61 (1979).
[7]John W. Palmour, U.S. Patent No. 4,875,083 (17 October 1989).
[8]A. Koudymov, X. Hu, K. Simin, G. Simin, M. Ali, J. Yang, and M. A. Khan, IEEE Electron Device Lett. **23**, 449 (2002).
[9]A. Koudymov, S. Rai, V. Adivarahan, M. Gaevski, J. Yang, G. Simin, and M. A. Khan, IEEE Microw. Wirel. Compon. Lett. **14**, 560 (2004).
[10]G. Simin, A. Koudymov, Z.-J. Yang, V. Adivarahan, J. Yang, M. Asif Khan, IEEE Electron Device Lett. **26**, 56 (2005).
[11]Gregory Snider, computer code 1D POISSON/SCHRODINGER SOLVER (University of Notre Dame, http://www.nd.edu/~gsnider/).
[12]O. Ambacher, B. Foutz, J. Smart, J. R. Shealy, N. G. Weimann, K. Chu, M. Murphy, A. J. Sierakowski, W. J. Schaff, L. F. Eastman, R. Dimitrov, A. Mitchell, and M. Stutzmann, J. Appl. Phys. **87**, 334 (2000).
[13]S. Rumyantsev, M. S. Shur, R. Gaska, M. Levinshtein, M. A. Khan, G. Simin, and J. Yang, Int. J. High Speed Electron. Syst. **12**, 449 (2002).
[14]M. A. Khan, A. Tarakji, H. Fatima, X. Hu, J. P. Zhang, G. Simin, M. S. Shur, and R. Gaska, IEEE Electron Device Lett. **24**, 369 (2003).